Optical induction of plasticity at single synapses reveals input-specific accumulation of αCaMKII

Yan-Ping Zhang, Niklaus Holbro, and Thomas G. Oertner*

Friedrich Miescher Institute, Maulbeerstrasse 66, CH-4058 Basel, Switzerland

Long-term potentiation (LTP), a form of synaptic plasticity, is a primary experimental model for understanding learning and memory formation. Here, we use light-activated channelrhodopsin-2 (ChR2) as a tool to study the molecular events that occur in dendritic spines of CA1 pyramidal cells during LTP induction. Two-photon uncaging of MNI-glutamate allowed us to selectively activate excitatory synapses on optically identified spines while ChR2 provided independent control of postsynaptic depolarization by blue light. Pairing of these optical stimuli induced lasting increase of spine volume and triggered translocation of αCaMKII to the stimulated spines. No changes in αCaMKII concentration or cytoplasmic volume were observed in neighboring spines on the same dendrite, providing evidence that αCaMKII accumulation at postsynaptic sites is a synapse-specific memory trace of coincident activity.

channelrhodopsin-2 | dendritic spines | synaptic plasticity | two-photon uncaging | MNI-glutamate

Activity-dependent changes in synaptic strength are generally considered to be the cellular basis of learning and memory (1). Long-term potentiation (LTP), the most extensively studied form of such synaptic plasticity, can be triggered within seconds by coincident activity in presynaptic and postsynaptic cells. The possible structural modifications that occur at synapses where LTP has been induced are poorly known because of the difficulty of simultaneously measuring functional and morphological parameters at individual synapses. Furthermore, it is controversial whether neighboring synapses can be modified independently (2–4). In a recent report, it has been shown that spatially clustered synapses can cooperate in the induction of plasticity and that cytoplasmic factors are responsible for this functional cross-talk (5). The identity of these diffusible factors, however, has not been clarified.

A key player in the LTP signaling cascade is αCaMKII, which is thought to function as a molecular switch: Following activation by Ca^{2+}-calmodulin, it can stay active for prolonged periods of time via autophosphorylation (6, 7). Reports that brief application of glutamate or NMDA to cultured hippocampal neurons induces CaMKII accumulation in spines (8–10) have created much interest because αCaMKII activation is both necessary and sufficient to induce synaptic plasticity (6, 11). It has been suggested that postsynaptic accumulation of αCaMKII could be responsible for the synapse-specificity of LTP, because it localizes the putative activated kinase close to its substrates, e.g., AMPA receptors (7, 12) and protects it from dephosphorylation (13). However, a crucial prediction of this hypothesis, namely that αCaMKII accumulates specifically and exclusively at synapses that undergo LTP, has never been tested experimentally.

To address whether αCaMKII accumulates specifically in spines experiencing coincident activity, we developed an all-optical pairing protocol to induce synaptic plasticity at identified spines, combining two-photon uncaging of MNI-glutamate (14) with postsynaptic channelrhodopsin-2 (ChR2) activation. Thus, we could avoid the washout problems typically associated with whole-cell patch clamp [see supporting information (SI) Fig. S1] while maintaining precise temporal control over the postsynaptic

depolarization. Spine morphology and αCaMKII concentration were monitored by two-photon ratiometric measurements. We show that paired stimulation of a single synapse can induce long-lasting αCaMKII accumulation at that synapse, but not at neighboring spines that were not exposed to glutamate.

Results

Novel Strategy for Non-Invasive LTP Induction. In the classical electrophysiological pairing protocol, presynaptic action potentials are paired with postsynaptic depolarization that is provided by current injection via a somatic patch electrode (15). Using this technique, plasticity has to be induced within 5–10 min after break-in, because important signaling molecules, e.g., CaMKII, are rapidly washed out (Fig. S1). Because our goal was to optically monitor the concentration of fluorescently labeled αCaMKII during the induction of plasticity, it was essential not to disturb the cytoplasm during the experiment. We therefore used the light-gated cation channel channelrhodopsin-2 (ChR2) (16) to depolarize individual postsynaptic cells in a noninvasive fashion.

Comparing protein concentrations in dendrites and spines presented a second challenge. Most dendritic spines were substantially smaller than the point spread function of our microscope. As a result, the fluorescence intensity of labeled αCaMKII in individual spines was determined by two unknown variables: The concentration of αCaMKII in the spine and the volume of that spine. Thus, fluorescence intensity measurements in a single-color channel were not sufficient to quantify differences in protein concentration between spines and dendrites. We solved this problem by cotransfection with a freely diffusible dimeric RFP, which served as a marker of cytosolic volume. We then used a ratiometric approach (green/red fluorescence intensity ratio) to compare the concentration of αCaMKII in spines of different size. The level of αCaMKII overexpression was generally low in our experiments (≈13% of endogenous αCaMKII, Fig. S2).

A fluorescently labeled version of ChR2 would have resulted in staining of the cell membrane and thus interfered with our αCaMKII measurements. To assess the expression level of ChR2 in individual cells, we combined unlabeled ChR2 and soluble RFP in a single plasmid with separate promoters, which resulted in very reliable coexpression (see SI Text). Using particle-mediated gene transfer, we cotransfected hippocampal neurons with two vectors encoding three different proteins: ChR2/RFP and Dronpa-αCaMKII (Fig. 1a). In response to blue light illumination (200 ms, 470 nm LED), transfected cells produced

NEUROSCIENCE

Fig. 1. LTP induction by pairing of single action potentials in CA3 cells with ChR2-mediated depolarization of synaptically connected CA1 cells. (*a*) CA1 pyramidal cell in organotypic slice culture (maximum intensity projection) expressing ChR2, RFP, and Dronpa-α CaMKII. Arrows indicate SV40 polyA sequences. (*b*) Paired recording configuration to assess light-induced plasticity in transfected CA1 pyramidal cell. Blue spot indicates illuminated area. (*c*) LTP induction protocol. A single AP evoked by current injection (2 nA, 5 ms) into a patch-clamped CA3 pyramidal cell was paired with a short burst of 5 APs elicited by blue light illumination (200 ms) of a transfected CA1 pyramidal cell (Δt = 6 ms). Pairing was repeated 20 times at 0.1 Hz. (*d*) Light-induced bursting in postsynaptic cell (blue bar: 200 ms light pulses, 20 repetitions at 0.1 Hz) did not significantly change EPSC amplitudes in transfected CA1 pyramidal cells (107% ± 16%, n = 7 pairs). Pairing stimulation as described in *c* induced 274% ± 76% potentiation (n = 7 pairs). Insert: example traces before and after light stimulation. Error bars indicate SEM.

large inward currents (1395 pA ± 115 pA at peak and 804 pA ± 89 pA at steady-state, n = 21). In current clamp mode, the same blue light stimulation induced robust spiking (5.4 ± 0.5 spikes, Fig. 1*c*).

We next examined whether the light stimulation technique could be used to induce long-term potentiation of Schaffer collateral synapses. We performed dual patch-clamp recordings of connected pairs of untransfected CA3 and transfected CA1 pyramidal cells (Fig. 1*b*). Our induction protocol consisted of repetitive pairing of single presynaptic action potentials in a single CA3 cell with brief postsynaptic bursts induced by 200 ms light pulses from a high-power blue LED (Fig. 1*c*). To compensate for the propagation delay from CA3 to CA1 (17), we started the light pulse with a delay of Δt = 6 ms relative to the presynaptic current injection. After 20 pairings at 0.1 Hz in current clamp, excitatory postsynaptic currents (EPSCs) increased to 274% ± 76% (Fig. 1*d*). Previously, we and others have

shown that light-induced spiking is accompanied by calcium influx through voltage-gated calcium channels and through ChR2 itself (17, 18). Therefore, it was important to test whether light-induced spiking could trigger synaptic plasticity in the absence of presynaptic activity. In control experiments in which repetitive blue light stimulation was not paired with presynaptic activation, postsynaptic response amplitudes remained unchanged (107% ± 16%, Fig. 1*d*). We conclude that coincident stimulation was needed to induce LTP on cells expressing ChR2 and αCaMKII, analogous to the classical electrophysiogical pairing protocol (17, 19, 20).

Spine Volume Changes Induced by Pairing of Glutamate Uncaging and Blue Light. Having established that postsynaptic depolarization by optical activation of ChR2 is sufficient for pairing-induced LTP, the next step was to replace the electrophysiological stimulation of CA3 axons by 2-photon glutamate uncaging at individual spines. For this purpose, we combined two Ti:Sapph lasers for simultaneous 2-photon uncaging and 2-photon imaging (Fig. 2*a*). Uncaging laser power (725 nm) was adjusted such that uncaging-evoked excitatory postsynaptic currents (uEPSCs) had amplitudes of 15.2 pA ± 1.8 pA (laser power, ≈50 mW, pulse duration, 0.5 ms), similar to spontaneous miniature EPSCs (mEPSC = 18 pA ± 3 pA, n = 7 cells, data not shown). To induce LTP at individual spines of transfected cells, we paired single glutamate uncaging pulses with 200 ms blue light pulses (20 pairings at 0.1 Hz, Δt = 0). In a set of cells that were not used for morphometric analysis, we verified by patch-clamp recording that this optical pairing protocol, but not glutamate uncaging *without* simultaneous ChR2 activation (20 pulses at 0.1 Hz), resulted in a lasting increase in uEPSC amplitude (Fig. 2*b*). To monitor spine morphology in 3D, we acquired stacks of 20 image planes at 5-min intervals. The integrated intensity of the spine head was used as a measure of spine volume (see *SI Text*). Stimulated spines responded with a rapid volume expansion by a factor of 2.4, on average (Fig. 2*c*). Spine volume partially decreased during the following 15 min, but most stimulated spines (11/16) remained enlarged 30–40 min after stimulation. In a separate set of control experiments, using identical pairing of blue light and uncaging laser pulses in the absence of MNI-glutamate, we did not detect any spine enlargement (Fig. 2*c*) and thus could rule out any unspecific effects induced by the uncaging laser pulse itself.

αCaMKII Concentration in Dendritic Spines. By calculating the fluorescence intensity ratio between GFP-αCaMKII and RFP on a pixel-by-pixel basis (G/R), we were able to compare the concentration of αCaMKII in spines of different size (Fig. 3*a*). To pool spine data from cells with different relative expression levels of GFP-αCaMKII and RFP, we normalized the G/R ratio in the spine by G/R ratio in the dendrite (S/D ratio). The S/D ratio is a measure of αCaMKII enrichment in spines independent of spine volume. Under baseline conditions, αCaMKII in spines was enriched by a factor of 1.32 relative to the dendrite (Fig. 3*b*), suggesting that ≈24% of total αCaMKII in spines was bound to postsynaptic sites (see *SI Methods*). To test for potential measurement artifacts because of the different signal-to-noise ratio in spines and dendrites, we also determined S/D ratios of soluble EGFP/RFP. S/D ratios were normally distributed with a mean of 1.01, indicating that our ratiometric approach was indeed volume independent.

An alternative method to distinguish bound and soluble fraction is fluorescence recovery after photobleaching (FRAP) (8). For these experiments, we cotransfected cells with RFP and YFP-αCaMKII, which could be readily bleached using 2-photon excitation at 910 nm. After a brief laser pulse that bleached 70–80% of the fluorescent molecules in the spine, fluorescence in the red color channel recovered rapidly (median τ = 0.28 s,
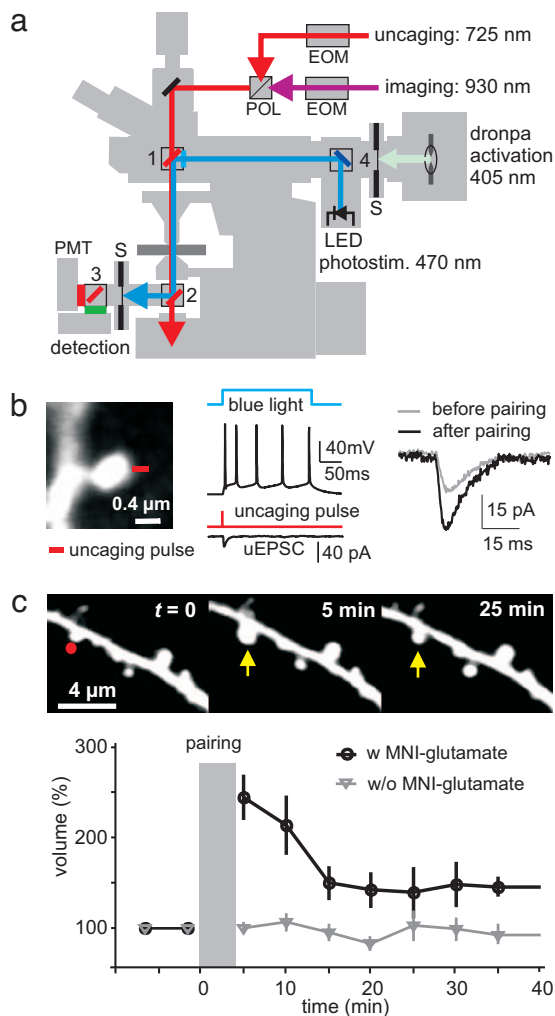
Fig. 2. Spine volume changes induced by pairing of glutamate uncaging and ChR2 activation. (*a*) Setup for simultaneous uncaging, imaging, and ChR2 stimulation. Two Ti:Sapph lasers were regulated by electro-optical modulators (EOM) and coupled through a polarizing beamsplitter cube (POL). A high-power blue LED coupled in through the epifluorescence port excited ChR2. Dichroic mirrors were 700DCXXR (1, 2), 560DCXR (3), and Q505LP (4). Photomultiplier tubes (PMT) were protected by a shutter (S) during the blue light pulses. (*b*) To induce plasticity at individual synapses, single uncaging pulses were paired with 200 ms blue light pulses 20 times at 0.1 Hz (Δ*t* = 0). uEPSCs are averages of five consecutive traces each. (*c*) Spine volume change induced by optical pairing protocol in the presence of MNI-glutamate (RFP signal, maximum projections). Time course shows transient and permanent component (black circles, *n* = 16 spines, 8 cells). No volume changes were induced in the absence of MNI-glutamate (gray triangles, *n* = 12 spines, 5 cells).

n = 80) to its initial value, indicating free diffusion of the dimeric RFP (Fig. 3*c*). YFP-αCaMKII fluorescence, however, did not fully recover, indicating a fraction of αCaMKII molecules that were bound to postsynaptic sites. To quantify the unrecoverable fraction, we fit a single exponential function to the normalized fluorescence recovery data $F(t)$:

$$F(t) = 1 - f_U - f_S e^{-\frac{t}{\tau}}$$

where f_U and f_S are the unrecoverable and soluble fraction of total αCaMKII, respectively, and τ is the recovery time constant. For wild-type YFP-αCaMKII, the unrecoverable fraction was 21% ± 12% (mean ± SD). To test whether binding depended on

the phosphorylation state of αCaMKII, we generated a double mutant (TT305/6VA) where two inhibitory autophosphorylation sites were removed. The threshold for kinase activation and for LTP induction is known to be lowered in the TT305/6VA mutant (21–23). Indeed, cells transfected with mutant αCaMKII had a significantly higher unrecoverable fraction of 42% ± 28% ($P < 0.05$). Time constants of recovery, however, were not significantly different for WT and mutant αCaMKII (median τ_{WT} = 12.5 s; τ_{TTVA} = 14.3 s), suggesting that the mobility of the soluble fraction was not influenced by the mutation. As expected, the S/D ratio and the unrecoverable fraction were correlated in individual spines, but individual measurements deviated from the expected relationship (curve in Fig. 3*d*). The deviation suggests that the assumption of a single, uniform population of bound αCaMKII molecules was probably an oversimplification. More likely, subpopulations of bound αCaMKII in the spine head turn over on multiple time scales (see ref. 36). On the basis of these considerations, we decided to rely on ratio measurements rather than on FRAP to assess the effects of LTP on αCaMKII binding.

Spine Enlargement Precedes the Input-Specific Accumulation of αCaMKII. αCaMKII translocation into spines after global chemical stimulation has been demonstrated previously (8, 24, 25). Here, our question was whether αCaMKII translocation is detectable, specific, and persistent following potentiation of a single synapse. A concern for optical concentration measurements of fluorescently labeled proteins is potential bleaching artifacts during time-lapse imaging and glutamate uncaging. To minimize this problem, we labeled αCaMKII with the photoswitchable GFP Dronpa-Green, which can be reactivated after bleaching by brief UV illumination (26). From a series of control experiments, we estimated that ≈95% of bleached Dronpa-αCaMKII was reactivated by low-power illumination at 405 nm (Fig. S3). We cotransfected CA1 pyramidal cells with Dronpa-αCaMKII, RFP, and unlabeled ChR2. Image stacks were obtained every 4 min, and Dronpa fluorescence was reactivated before each acquisition. We verified that UV illumination did not induce spiking of ChR2-transfected cells (Fig. S3). After optical LTP induction, the majority of spines (18/23 experiments) responded with a rapid increase in spine head volume. Ten of these 18 spines were still enlarged 30–40 min after stimulation (Fig. 4*a*, right example). Persistent spine enlargement has been linked previously to successful LTP induction at the spine synapse (2, 5). Therefore, we split our sample of stimulated spines in two different groups: spines that responded with a persistent volume increase to the pairing protocol and spines that did not (Fig. 4*b*). We also analyzed neighboring spines on the same dendrite that were not directly stimulated (average distance from the stimulated spine: 5.5 μm). We then compared αCaMKII enrichment (spine/dendrite) in the three groups (Fig. 4*c*). Only in the group of spines with persistent volume increases did we detect a significant increase in the concentration αCaMKII at *t* = 13 min after the onset of stimulation ($P < 0.05$, see also Fig. S4). Interestingly, all groups had the same αCaMKII concentration before stimulation, indicating that the initial αCaMKII level had no predictive value for the type of volume change (transient vs. persistent) induced by the pairing stimulation. In neighboring unstimulated spines, we did not detect an increase in αCaMKII concentration, indicating high spatial specificity of αCaMKII enrichment. We noted that spine enlargement preceded the input-specific accumulation of αCaMKII: Whereas spine volume reached its maximum immediately after stimulation, αCaMKII concentration reached its peak ≈10 min later. Using the spine/dendrite ratio before stimulation as a starting point, we calculated changes in the amount of bound and soluble αCaMKII in stimulated and nonstimulated spines (Fig. 4*d*). This analysis revealed that in the
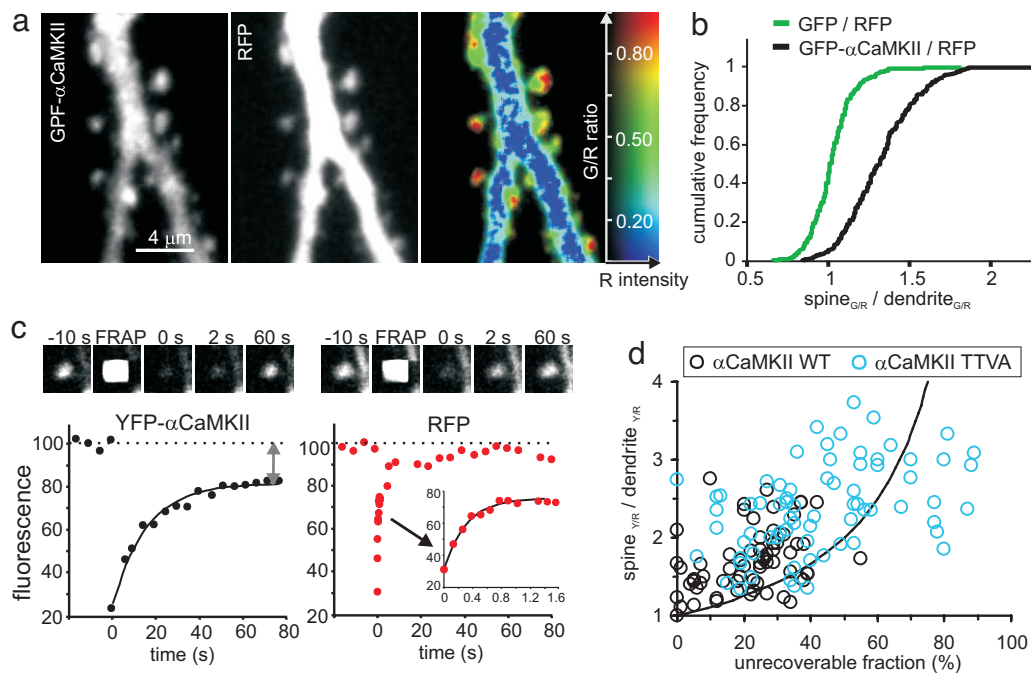
Fig. 3. Enrichment of αCaMKII in spines. (*a*) CA1 pyramidal cell dendrite expressing GFP-αCaMKII and RFP (maximum intensity projections, grayscale saturated to show dim spines). Left: GFP-αCaMKII signal. Middle: Cytoplasmic volume (RFP). Right: Color-coded ratio of αCaMKII/volume (G/R), indicating elevated αCaMKII concentration in spines. (*b*) Cumulative distribution of G/R ratio (protein concentration) in spines relative to parent dendrite (S/D ratio). αCaMKII, but not GFP, is enriched in dendritic spines. GFP, $n = 286$ spines, 3 cells, median S/D ratio = 1.01; GFP-αCaMKII, $n = 80$ spines, 4 cells, median S/D ratio = 1.32. (*c*) FRAP analysis on a dendritic spine expressing YFP-αCaMKII and RFP. Black dots: YFP-αCaMKII fluorescence intensity in spine. Black line: single exponential fit. Note ≈20% unrecoverable fraction. Red dots: RFP fluorescence. Note rapid (insert) and complete recovery of fluorescence. RFP showed much faster recovery following photobleaching than YFP-αCaMKII ($\tau_{RFP} = 0.31$ s, $\tau_{YFP-\alpha CaMKII} = 16$ s). (*d*) Correlation between FRAP and spine/dendrite (s/d) ratio measurements in individual spines. YFP-αCaMKII TT305/306VA mutant showed higher unrecoverable fraction (f_u) and higher enrichment in spines compared with wild-type αCaMKII. Black line: predicted correlation $f_u = 1 - 1/(s/d)$.

spines with a persistent increase in volume, the *absolute amount* of bound αCaMKII in the spine had approximately doubled 30–40 min after stimulation. The bound *fraction*, however, peaked transiently ≈10 min after stimulation, but later returned to baseline (29% before stimulation, 33% 30–40 min after stimulation). These experiments suggest that paired stimulation moved 10 of 23 spines to a new stable state, characterized by an increased amount of both soluble and bound αCaMKII and a larger volume. No significant volume or αCaMKII changes were detected in neighboring spines on the same dendrite.

Induction of Long-Term Plasticity by Synaptic Activation. Glutamate uncaging is a convenient way to stimulate individual dendritic spines, but the glutamate concentration in the synaptic cleft depends on intensity and duration of the laser pulse (5). If our observations following optical pairing (Figs. 3 and 4) were indeed characteristic for LTP, similar changes would be expected following high frequency electrical activation of Schaffer collaterals, another well established LTP induction protocol. To identify synaptically stimulated spines, we used post hoc calcium imaging: First, spiny dendrites of transfected CA1 pyramidal cells were imaged while stimulating Schaffer collateral axons at high frequency (3 × 1 s, 100 Hz). After time-lapse imaging of a transfected cell for ≈40 min, we patch clamped the same cell to infuse a calcium sensitive dye (Fluo 4FF) and Alexa-Fluor 594. Although the plasticity-inducing tetanic stimulation was applied under blind conditions, we could reactivate the same set of synapses by applying short bursts (3 APs) to the stimulation electrode. In four experiments, we successfully identified synaptically stimulated spines by post hoc Ca²⁺ imaging (Fig. S5). Analysis of the volume-filling RFP fluorescence in the synaptically stimulated spines revealed that the LTP protocol induced

a rapid volume increase with a large persistent component. The total amount of αCaMKII also increased in the stimulated spines, peaking 5 min after stimulation. Analysis of the soluble and bound fraction in the tetanized spines revealed that 25–35 min after stimulation, the amount of bound αCaMKII was increased by a factor of 2.0 (Fig. S5). In summary, the physiological and morphological consequences of high-frequency stimulation were remarkably similar to the changes we observed after pairing of glutamate uncaging with postsynaptic depolarization by ChR2. This indicates that persistent spine volume increase and synapse-specific binding of αCaMKII are hallmarks of LTP in CA1 pyramidal neurons.

Discussion

Here, we show that paired activation of a single synapse on a single cell leads to long-lasting enrichment of αCaMKII at that synapse. Our study highlights several advantages of plasticity induction by optical pairing. Unlike chemical LTP and zero Mg²⁺ protocols (25, 27, 28), optical pairing does not lead to unspecific activation of the entire tissue. Therefore, activity-induced changes at individual synapses can be studied in an unperturbed cellular environment. The spatial resolution is clearly superior to local perfusion approaches, which have been used previously to probe the input specificity of LTP and CaMKII translocation (4, 23). Degrading electrical access or cell health, which limits the duration of electrophysiological recordings, is not an issue in the all-optical experiments. Most importantly, the intracellular milieu of the postsynaptic cell is not affected, permitting detection of subtle changes in protein concentration.

Two previous studies have established the tight correlation between lasting increases in spine volume and LTP of uncaging-
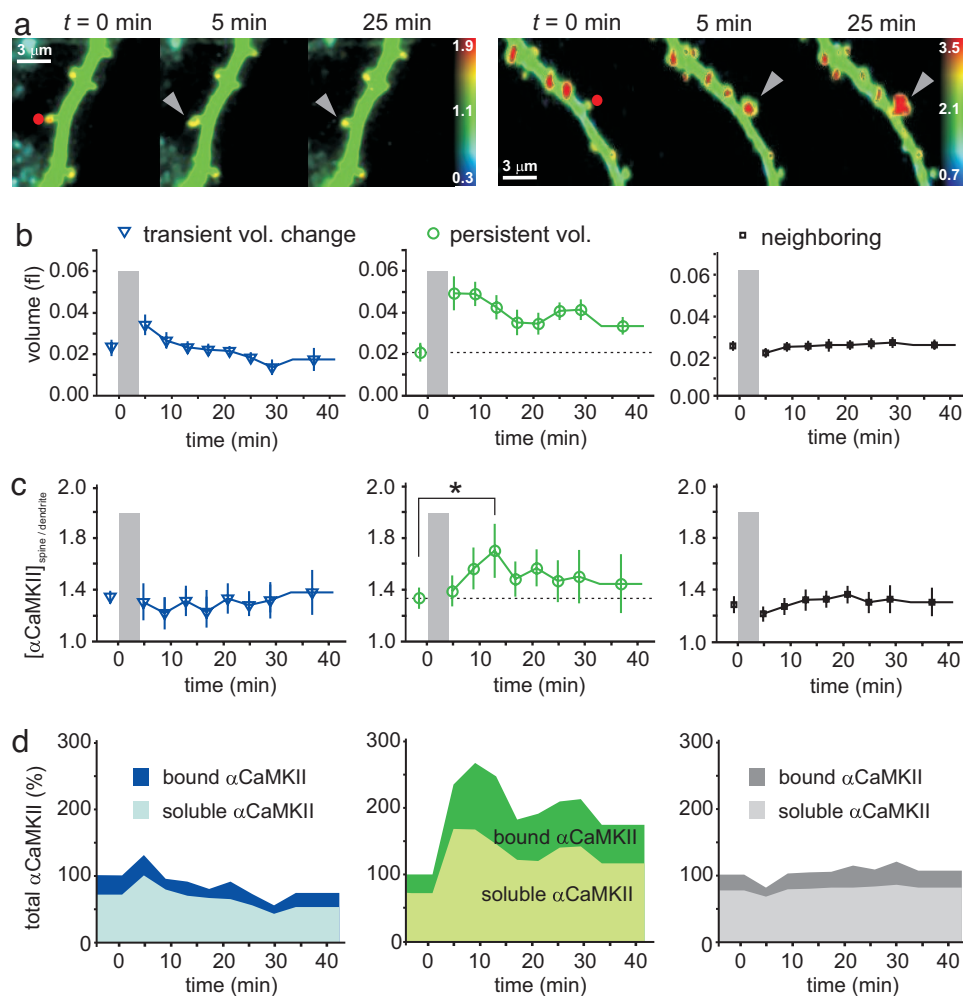
Fig. 4. Input-specific accumulation of αCaMKII. (*a*) Maps of αCaMKII concentration. Stimulated spines (red dot) showed either transient (left) or persistent increase in volume and αCaMKII concentration (right). (*b*) Spine volume changes in response to optical pairing protocol. Stimulated spines were sorted into two groups according to their volume 30–40 min after pairing (transient spines: <30% change, n = 13; persistent spines, >30% change, n = 10). Right panel: neighboring, nonstimulated spines on the same dendrite show no significant volume change (mean distance from stimulated spine: 5.5 μm ± 0.9 μm, n = 110). (*c*) αCaMKII enrichment in spines: αCaMKII concentration (G/R) in spine normalized by αCaMKII concentration (G/R) in dendrite. Spines were sorted according to persistence of volume change as described in *b*. Significant αCaMKII enrichment was detected in persistently enlarged spines at *t* = 13 min (paired *t* test, one-tailed, $P < 0.05$), but not in the group that responded only with transient swelling. Note identical αCaMKII concentration in both groups before stimulation. Right panel: neighboring, nonstimulated spines showed no significant change in αCaMKII concentration. (*d*) Soluble and bound fraction calculated from data shown in *c* and *b* (see *SI Text*). In the spines that responded with persistent volume change to paired stimulation (middle panel), the amount of both bound and soluble αCaMKII was persistently increased by a factor of 2.0 and 1.6, respectively.

evoked EPSPs (2, 5). Moreover, spine shrinkage was reported following the induction of long-term depression (29). Here, we report lasting spine volume increase following LTP induction by tetanic activation of Schaffer collaterals (Fig. S5) and in response to optical pairing (Figs. 2 and 4). To minimize photodamage and bleaching in our pairing experiments, we used a relatively weak induction protocol (20 uncaging pulses at 0.1 Hz, 0.5 ms pulse duration, 3–5 postsynaptic APs) compared with previously used uncaging protocols [60 pulses at 1 Hz in zero Mg^{2+} solution (2); 30 pulses of 4 ms at 0.5 Hz, V_m = 0 mV (5)]. As expected, our protocol induced lasting volume increases only in a subset of spines. This variability in the plasticity of CA3-CA1 connections was also apparent in our electrophysiological experiments using the same number and frequency of paired stimulations (Fig. 1*d*) and is consistent with previous studies (17, 19, 20). Because glutamate uncaging bypasses the presynaptic terminal, the differential sensitivity to optical pairing can be attributed to postsynaptic differences. We show that neither the initial spine volume nor the initial αCaMKII concentration

could be used to predict the response of a spine to pairing stimulation (Fig. 4 *b* and *c*). Nevertheless, optical pairing provides the first noninvasive approach to investigate which biological parameters control the threshold for plasticity induction at individual synapses.

Translocation of αCaMKII to postsynaptic sites has been previously reported after extracellular glutamate application or "chemical LTP" (8, 10, 23, 25). Here, our goal was to investigate whether this enrichment is restricted to synapses that experience plasticity-inducing stimulation. We show that the concentration of αCaMKII increased significantly only in those spines that underwent lasting volume changes (Fig. 4). High-frequency synaptic stimulation (100 Hz, 1 s) induced very similar increases in both soluble and bound αCaMKII (Fig. S5), indicating that αCaMKII enrichment was not an artifact of uncaging stimulation. Spines that were not directly stimulated sometimes increased or decreased their volume spontaneously, but on average, no significant αCaMKII loss or gain was detected. In a previous study, it has been shown that following plasticity

induction at individual spines, the threshold for LTP induction is lowered in neighboring spines (5). Although αCaMKII can maintain its activation state for some time by autophosphorylation and is thus a potential candidate for a short-range communication system (7), we found no indication of functional cross-talk between neighboring spines on the level of αCaMKII.

Given the time constant of αCaMKII diffusion measured in our FRAP experiments ($\tau = 12.5$ s), the αCaMKII increase in the stimulated spines was surprisingly slow. In a recent study, a rapid increase in the diffusional resistance of the spine neck following paired stimulation was reported (30), which could conceivably slow down diffusion of a large protein like CaMKII and thus limit the number of CaMKII molecules available for binding. A second possibility is the slow generation of additional binding sites for αCaMKII by structural enlargement of the PSD in the first 5–10 min following potentiation. Interestingly, a similarly protracted time course was reported for the AMPA receptor subunit GluR1 in a previous study, peaking 6 min after induction of chemical LTP (31). The similar time course and the persistent, 2-fold increase in the amount of bound αCaMKII we report here is consistent with a structural role of αCaMKII in anchoring glutamate receptors to the postsynaptic density (7, 32, 33). Under baseline conditions, the *amount* of bound αCaMKII correlates with spine size and synaptic strength, but the *ratio* between bound and soluble αCaMKII does not (33). This static picture can be understood in the light of our time-resolved study, where we show that 30–40 min after the potentiation event, the equilibrium between bound and soluble αCaMKII returned to values close to the baseline level, but the absolute amount of

αCaMKII in potentiated spines had doubled (Fig. 4d, Fig. S5). For the inhibition-deficient mutant TT305/6VA, we measured a significantly higher ratio of bound to soluble αCaMKII (Fig. 3d), indicating that this ratio depends on the level of αCaMKII activation in the spine. Recently, it has been demonstrated that LTP can be partially reversed by blocking CaMKII activity, providing evidence for its role in the maintenance of synaptic strength (34). In summary, the insertion of additional AMPA receptors, which is the accepted structural correlate of LTP at Schaffer collateral synapses (2), seems to be linked with a lasting increase in spine volume and binding of additional αCaMKII to postsynaptic sites. Here, we show that these changes can be induced with single-spine specificity, validating Hebb's postulate on the micrometer scale.

Methods

Plasmid Construction. We constructed a single plasmid for neuron-specific coexpression of ChR2-YFP (K. Deisseroth) and dimeric RFP (tdimer2, R. Y. Tsien). Details are provided in *SI Text*.

Slice Culture and Electrophysiology. Organotypic hippocampal slices were prepared from Wistar rats at postnatal day 5 as described in ref. 35, in accordance with the animal care and use guidelines of the Veterinary Department Basel-Stadt. Patch-clamp recordings were performed at 30–32°C as described in *SI Text*.

1. Bliss TV, Collingridge GL (1993) A synaptic model of memory: Long-term potentiation in the hippocampus. *Nature* 361:31–39.
2. Matsuzaki M, Honkura N, Ellis-Davies GC, Kasai H (2004) Structural basis of long-term potentiation in single dendritic spines. *Nature* 429:761–766.
3. Bi G, Poo M (2001) Synaptic modification by correlated activity: Hebb's postulate revisited. *Annu Rev Neurosci* 24:139–166.
4. Engert F, Bonhoeffer T (1997) Synapse specificity of long-term potentiation breaks down at short distances. *Nature* 388:279–284.
5. Harvey, CD, Svoboda, K (2007) Locally dynamic synaptic learning rules in pyramidal neuron dendrites *Nature* 450:1195–1200.
6. Giese KP, Fedorov NB, Filipkowski RK, Silva AJ (1998) Autophosphorylation at Thr286 of the alpha calcium-calmodulin kinase II in LTP and learning. *Science* 279:870–873.
7. Lisman JE, Zhabotinsky AM (2001) A model of synaptic memory: A CaMKII/PP1 switch that potentiates transmission by organizing an AMPA receptor anchoring assembly. *Neuron* 31:191–201.
8. Shen K, Meyer T (1999) Dynamic control of CaMKII translocation and localization in hippocampal neurons by NMDA receptor stimulation. *Science* 284:162–166.
9. Shen K, Teruel MN, Connor JH, Shenolikar S, Meyer T (2000) Molecular memory by reversible translocation of calcium/calmodulin-dependent protein kinase II. *Nat Neurosci* 3:881–886.
10. Merrill MA, Chen Y, Strack S, Hell JW (2005) Activity-driven postsynaptic translocation of CaMKII. *Trends Pharmacol Sci* 26:645–653.
11. Lledo PM, Hjelmstad GO, Mukherji S, Soderling TR, Malenka RC, et al. (1995) Calcium/calmodulin-dependent kinase II and long-term potentiation enhance synaptic transmission by the same mechanism. *Proc Natl Acad Sci USA* 92:11175–11179.
12. Soderling TR, Derkach VA (2000) Postsynaptic protein phosphorylation and LTP. *Trends Neurosci* 23:75–80.
13. Mullasseril P, Dosemeci A, Lisman JE, Griffith LC (2007) A structural mechanism for maintaining the 'on-state' of the CaMKII memory switch in the post-synaptic density. *J Neurochem* 103:357–364.
14. Matsuzaki M, Ellis-Davies GC, Nemoto T, Miyashita Y, Iino M, et al. (2001) Dendritic spine geometry is critical for AMPA receptor expression in hippocampal CA1 pyramidal neurons. *Nat Neurosci* 4:1086–1092.
15. Chen HX, Otmakhov N, Lisman J (1999) Requirements for LTP induction by pairing in hippocampal CA1 pyramidal cells. *J Neurophysiol* 82:526–532.
16. Boyden ES, Zhang F, Bamberg E, Nagel G, Deisseroth K (2005) Millisecond-timescale, genetically targeted optical control of neural activity. *Nat Neurosci* 8:1263–1268.
17. Zhang YP, Oertner TG (2007) Optical induction of synaptic plasticity using a light-sensitive channel. *Nat Meth* 4:139–141.
18. Nagel G, Szellas T, Huhn W, Kateriya S, Adeishvili N, et al. (2003) Channelrhodopsin-2, a directly light-gated cation-selective membrane channel. *Proc Natl Acad Sci USA* 100:13940–13945.
19. Petersen CC, Malenka RC, Nicoll RA, Hopfield JJ (1998) All-or-none potentiation at CA3-CA1 synapses. *Proc Natl Acad Sci USA* 95:4732–4737.
20. Debanne D, Gahwiler BH, Thompson SM (1999) Heterogeneity of synaptic plasticity at unitary CA3-CA1 and CA3-CA3 connections in rat hippocampal slice cultures. *J Neurosci* 19:10664–10671.
21. Hanson PI, Schulman H (1992) Inhibitory autophosphorylation of multifunctional Ca^{2+}/calmodulin-dependent protein kinase analyzed by site-directed mutagenesis. *J Biol Chem* 267:17216–17224.
22. Elgersma Y, Fedorov NB, Ikonen S, Choi ES, Elgersma M, et al. (2002) Inhibitory autophosphorylation of CaMKII controls PSD association, plasticity, and learning. *Neuron* 36:493–505.
23. Thalhammer A, Rudhard Y, Tigaret CM, Volynski KE, Rusakov DA, et al. (2006) CaMKII translocation requires local NMDA receptor-mediated Ca^{2+} signaling. *EMBO J* 25:5873–5883.
24. Bayer KU, LeBel E, McDonald GL, O'Leary H, Schulman H, et al. (2006) Transition from reversible to persistent binding of CaMKII to postsynaptic sites and NR2B. *J Neurosci* 26:1164–1174.
25. Otmakhov N, Tao-Cheng JH, Carpenter S, Asrican B, Dosemeci A, et al. (2004) Persistent accumulation of calcium/calmodulin-dependent protein kinase II in dendritic spines after induction of NMDA receptor-dependent chemical long-term potentiation. *J Neurosci* 24:9324–9331.
26. Ando R, Mizuno H, Miyawaki A (2004) Regulated fast nucleocytoplasmic shuttling observed by reversible protein highlighting. *Science* 306:1370–1373.
27. Sharma K, Fong DK, Craig AM (2006) Postsynaptic protein mobility in dendritic spines: Long-term regulation by synaptic NMDA receptor activation. *Mol Cell Neurosci* 31:702–712.
28. Fong DK, Rao A, Crump FT, Craig AM (2002) Rapid synaptic remodeling by protein kinase C: Reciprocal translocation of NMDA receptors and calcium/calmodulin-dependent kinase II. *J Neurosci* 22:2153–2164.
29. Zhou Q, Homma KJ, Poo MM (2004) Shrinkage of dendritic spines associated with long-term depression of hippocampal synapses. *Neuron* 44:749–757.
30. Bloodgood BL, Sabatini BL (2005) Neuronal activity regulates diffusion across the neck of dendritic spines. *Science* 310:866–869.
31. Kopec CD, Li B, Wei W, Boehm J, Malinow R (2006) Glutamate receptor exocytosis and spine enlargement during chemically induced long-term potentiation. *J Neurosci* 26:2000–2009.
32. Hayashi Y, Shi SH, Esteban JA, Piccini A, Poncer JC, et al. (2000) Driving AMPA receptors into synapses by LTP and CaMKII: Requirement for GluR1 and PDZ domain interaction. *Science* 287:2262–2267.
33. Asrican B, Lisman J, Otmakhov N (2007) Synaptic strength of individual spines correlates with bound Ca^{2+}-calmodulin-dependent kinase II. *J Neurosci* 27:14007–14011.
34. Sanhueza M, McIntyre CC, Lisman JE (2007) Reversal of synaptic memory by Ca^{2+}/calmodulin-dependent protein kinase II inhibitor. *J Neurosci* 27:5190–5199.
35. Stoppini L, Buchs PA, Muller D (1991) A simple method for organotypic cultures of nervous tissue. *J Neurosci Meth* 37:173–182.
36. Otmakhov N, et al. (2007) *Soc Neurosci* 788.8 (abstr).

Zhang *et al.*